JOURNAL OF AIRCRAFT
Vol. 32, No. 5, September–October 1995

Inverse Method for Airfoil Design

Alejandro C. Limache*
Universidad Nacional de Córdoba, Córdoba 5000, Argentina

This article presents an exact inverse method that generates the airfoil shape, satisfying all fluid dynamic and geometric constraints imposed by prescribing any input velocity distribution (or contour at the hodograph), with the only restriction that it does not take the same vector velocity at two different points of the boundary. The method is supported with a successive conformal mapping technique that can also be used in other problems as the one of grid-generation. The method may be a valuable general tool to obtain optimized designs with excellent performance. It can be extended to generate high-lift airfoils for compressible subsonic flow velocities.

Nomenclature

C_L = lift coefficient
C_p = pressure coefficient
$h(R_w)$ = image of a region R_w by the analytic function h
l_n = complex logarithm
P, P_z = analytic functions that define the complex potential W of a flow W in a region R_Z and R_z, respectively
p = pressure
q = modulus of the velocity
$\mathbf{q}$ = velocity vector
q_0 = speed of the freestream incident on the circular obstacle in the z plane
q_∞ = modulus of the freestream design velocity incident on the designed airfoil
R = radius of the circular obstacle in the z plane
R_V = region in the V plane that contains all the complex velocity values taken; its boundary is the velocity contour
R_Z = region of the Z plane whose boundary defines the physical obstacle(s) around which the fluid flows; here, it is the region around the designed airfoil
R_z = region of the z plane whose boundary is defined by nonphysical obstacle(s) around which a fluid flows; here, it is the region exterior to a circular obstacle
$R_{\xi 1}, R_{\xi 2}, \ldots$ = regions in the ξ_1 plane, ξ_2 plane, . . . , respectively, determined by the successive mapping (by $G_1^{-1}, G_2^{-1}, \ldots$) of the region R_V until its transformation onto the region R_z
S = forward stagnation point on the airfoil
T = trailing edge of the airfoil
U = unitary circular disc
u, v = X and Y component of the velocity
V = complex velocity, $qe^{-i\theta}$
V_f = image by G_V of the point z_f
V plane or hodograph = complex plane where one represents the values of the complex velocity, $u - iv$
V_∞ = freestream complex velocity of the design, $q_\infty e^{-i\theta_\infty}$
w = generic complex variable
$\bar{w}$ = complex conjugate of w
w_S, w_T = points in the w plane that correspond to the points S and T on the airfoil, respectively (for example, V_T is the point in the V plane that defines the velocity of T)
Z = complex variable whose components X, Y define the coordinates of a two-dimensional physical plane
z = complex variable whose components x, y define a two-dimensional plane with a circular obstacle centered at the origin
z_f, z_0 = particular complex points in the z plane that correspond to the particular points Z_f and Z_0 in the Z plane
α = angle of the freestream incident on the circular obstacle (z plane)
Γ = circulation
θ = direction of the velocity
θ_∞ = direction of the freestream design velocity incident on the designed airfoil
ξ_j = complex variable that defines an auxiliary ξ_j plane, $j = 1, 2, 3, 4$
ρ = density
ψ, φ, W = stream function, velocity potential, and complex potential of the flow, respectively

Introduction

INVERSE methods of airfoil design have received the attention of a lot of researchers. Four representative studies are those of Lighthill,[1] Strand,[2] Cohen,[3] and Volpe.[4] The problem in airfoil design is finding a geometry that satisfies some prescribed dynamic (usually, a pressure distribution) or geometric features that provide the required behavior (usually

Received April 9, 1994; revision received Feb. 10, 1995; accepted for publication Feb. 28, 1995.

*Facultad de Matemática, Astronomía y Física.

maximum lift and minimum drag). This article presents a solution to the problem of finding a single airfoil that satisfies physically meaningful dynamic or geometric requirements imposed via prescribing a contour that defines the velocity on the airfoil surface. This contour is called velocity contour (VC) and will be more exactly defined in the following sections.

The method has been derived under the assumption of ideal flow. This approach is justified, if it is assumed that the flow remains attached everywhere. Compressibility can be accounted for by an extension of the method.

Since it is possible to incorporate the analysis and solution of the problem of separation of the boundary layer to the method, this inverse technique can be an effective tool in the design of useful and practical airfoils. In general, separation occurs at the pressure recovery zone on the tail end of the upper surface, and so this coupling can be achieved in the following ways:

1) Through an optimization of the velocity contour that insures the no-separation of the flow, as done by Liebeck[5,6] by means of imposing the Stratford–imminent separation criteria.[7] Then the mean value of the velocity of the flow along the deceleration zone is as large as possible subject to the constraint that the boundary layer does not separate.

2) Verifying the no-separation in the designed airfoil a posteriori by boundary-layer analysis. If the separation is detected, one can easily modify the velocity contour to reduce, where necessary, adverse pressure gradients and redesign the airfoil until acceptable results are obtained.

3) Finally, if one wants to preserve the shape of the distribution, energizing the boundary layer through jet blowing is effective.

The method uses as input the VC. Any prescribed VC will not necessarily imply a closed, and non-re-entrant airfoil. The latter condition can be checked after the determination of the airfoil. On the other hand, the closure condition and the viability of the design is verified before the design itself, by simply finding the solution of a unique complex equation. If one or both of these physical conditions is not met, the designer will have to modify the VC. This necessary modification is usually reduced to a variation of the velocity corresponding to the trailing edge of the airfoil.

Some advantages of the inverse method presented in this article are the following: 1) it is an exact method, 2) it does not need complicated numerical algorithms, 3) it is of general application, 4) its extension to the whole of the subsonic compressible domain does not involve significant complications, and 5) it can be used to generate families of high-lift airfoils; for example, airfoils with flat rooftop configurations. Since the flat rooftop airfoils have optimized velocity distributions, they are inherently high-lift and potentially low-drag devices.

Two-Dimensional Ideal Flow Theory Applied to the Inverse Method Problem

Consider the motion of an ideal flow in a region R_Z as specified by the velocity vector $\boldsymbol{q}$ of the fluid at the point X, Y. The flow can be defined alternatively by an analytic function P

$$W = P(Z) = \varphi(X, Y) + i\psi(X, Y) \tag{1}$$

on R_Z as follows. The complex derivative $\mathrm{d}W/\mathrm{d}Z$ of W is the complex velocity, and satisfies

$$V = \frac{\mathrm{d}W}{\mathrm{d}Z} = \frac{\mathrm{d}P(Z)}{\mathrm{d}Z} = u(X, Y) - iv(X, Y) = qe^{-i\theta} \tag{2}$$

Since P, and $\mathrm{d}P/\mathrm{d}Z$ are analytic functions on R_Z, Eq. (2) defines a conformal mapping from the complex physical Z plane to the V plane. The region R_Z is mapped onto a region R_V in the V plane (see Fig. 1). It follows that the contour(s)

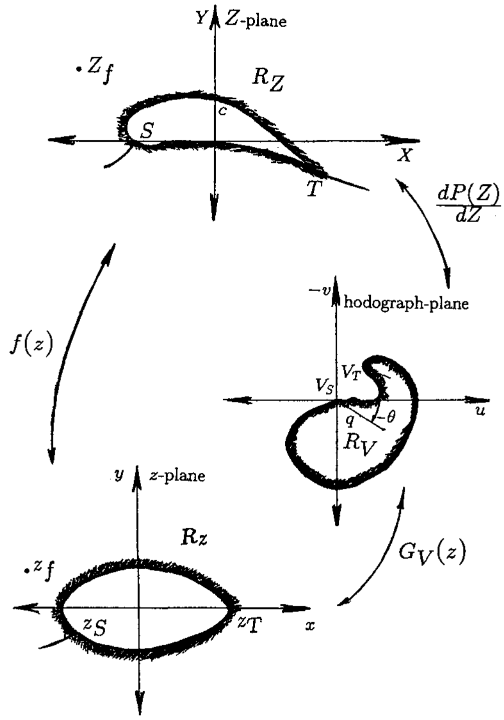

Fig. 1 Physical Z plane, the hodograph, and the z plane and their connection.

that defines the boundary of R_Z will be mapped into another contour(s) in the V plane. Then, this contour(s) in the hodograph V plane defines the velocities of the flow on the boundary of the obstacle(s) or airfoil(s) in the Z plane and is called velocity contour, or simply, VC.

Assume that $W = P(Z)$ defines the motion of an ideal flow; complex function theory shows that if an analytic function f maps one-to-one, a region R_z of a complex z plane onto the region R_Z, that is to say if

$$Z = f(z) \tag{3}$$

then the transformation f defines an analytic function on R_z

$$W = P_z(z) = P[f(z)] \tag{4}$$

and the new function can be interpreted as the complex potential of a flow in the region R_z. It is thus possible to determine the complex velocity of this flow in the region R_z by

$$\frac{\mathrm{d}W}{\mathrm{d}z} = \frac{\mathrm{d}P_z(z)}{\mathrm{d}z} \tag{5}$$

Finally, the complex velocity V in the physical Z plane can be expressed in terms of z:

$$V = \frac{\mathrm{d}W}{\mathrm{d}Z} = \frac{\mathrm{d}W}{\mathrm{d}z}\cdot\frac{\mathrm{d}z}{\mathrm{d}Z} = \frac{\mathrm{d}P_z(z)}{\mathrm{d}z}\cdot\left[\frac{\mathrm{d}f(z)}{\mathrm{d}z}\right]^{-1} \tag{6}$$

Writing $G_V(z)$ for the last term in this equation, one has

$$V = G_V(z) \tag{7}$$

Thus, G_V defines an analytic function that maps the region R_z of the z plane onto the region R_V of the hodograph V plane, as shown in Fig. 1. Finally, from the connection between z and Z, one deduces that the boundary of R_z will be mapped by G_V onto the VC.

Equations (3) and (7) present the implicit solution of any inverse problem. The problem will be solved if given some

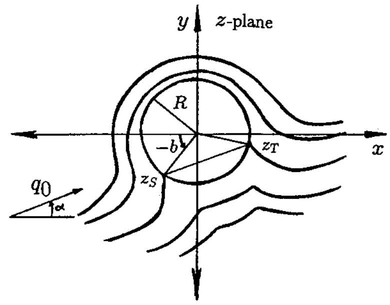

Fig. 2 Flow around a circular obstacle.

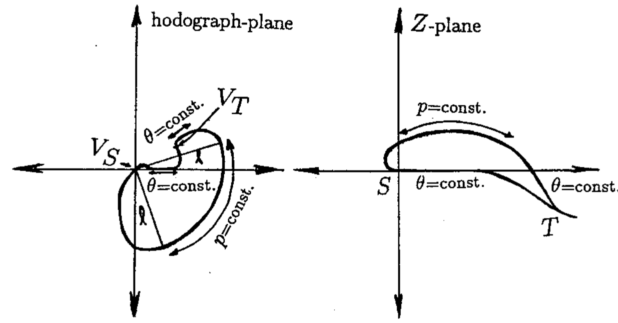

Fig. 3 Velocity contour and its corresponding rooftop airfoil.

region R_z in some z plane, it is then possible to determine the function f. To see that this is true, observe that to each value of a point z_f of the boundary of R_z, one finds a corresponding $Z_f = f(z_f)$ on the boundary of R_Z, which is the airfoil. It will be seen that f is expressed as an integral, where the integrand contains information deduced from the VC.

In what follows, use will be made of the most general ideal flow motion around a circular obstacle inside a uniform stream (see Fig. 2), as given by

$$W = P_z(z) = q_0 e^{-i\alpha} z + q_0 e^{i\alpha} R^2 \frac{1}{z} + \frac{\Gamma}{2\pi i} \ln z \qquad (8)$$

$$\frac{dW}{dz} = \frac{dP_z(z)}{dz} = q_0 e^{-i\alpha} - q_0 e^{i\alpha} R^2 \frac{1}{z^2} + \frac{\Gamma}{2\pi i} \frac{1}{z} \qquad (9)$$

VC: The Data Required for the Present Inverse Method

As mentioned in the Introduction, in airfoil design one needs to find an airfoil that meets certain requirements. These are usually of two kinds: 1) dynamic: to generate a prescribed pressure p along different components or sections of the airfoil and 2) geometric: that the contours of these sections have prescribed curvatures. Generally, a combination of both types is imposed.

Because the dynamic information about the pressure p can be given by the magnitude q of the velocity, and the geometric information can be imposed on the contour, by the value of θ, one can take into account both requirements by prescribing continuously in the hodograph plane the complex velocity $V = qe^{-i\theta}$ (see Fig. 3). Then, all the information is contained in the VC in the hodograph V plane.

This VC is the input of the inverse method presented here, and so it is convenient to elaborate on this.

1) The airfoil is designed to operate in a steady flow generated by a uniform stream. This is a basic assumption and has to be accounted for in establishing the VC.

2) For a given incidence θ_∞ of the uniform stream there are over any airfoil a point S of forward stagnation or impact-point and a detachment-point corresponding to the trailing edge T. The streamline that arrives at S separates in two streamlines, which meet in T. Since the complex velocity V_S of S is 0, the VC has to pass through the origin of the hodograph plane. On the other hand, the method imposes no restrictions on V_T.

3) To design the VC one has to have in mind at least a rough draft of the airfoil. Then the path, corresponding, e.g., the lower streamline, is followed; beginning with $V_S = 0$ and according to the requirements that one has over this section, one proceeds to define the VC until the point V_T corresponding to T is reached. Then one does the same for the route S-T corresponding to the upper streamline beginning again at the origin of the hodograph plane.

4) Figure 3 shows an example on the latter point, for the case of designing rooftop airfoils.

5) If there are no requirements on certain zones, one interpolates the VC between the established zones so as to obtain a continuous contour.

Finally, as will be seen later, the specification of the VC is a sufficient condition for the determination of f and, thus, of the corresponding airfoil. The problem is thus well posed when the designer specifies the VC.

General Implicit Solution of the Inverse Problem

Remembering the first equality of Eq. (2)

$$V = \frac{dW}{dZ}$$

an infinitesimal displacement dZ in the physical plane can be written as

$$dZ = \frac{1}{V} dW \qquad (10)$$

The displacement dZ can be expressed in terms of its corresponding displacement dz in an auxiliary z plane. Applying the chain rule to Eq. (10), one has

$$dZ = \frac{1}{V} \cdot \frac{dW}{dz} dz$$

Integrating this along any contour

$$Z_f = f(z_f) = \int_{z_0}^{z_f} \frac{1}{V} \cdot \frac{dW}{dz} dz \qquad (11)$$

where z_0 has been chosen as the point in the z plane corresponding to the point $Z_0 = 0$ in the Z plane.

In order to calculate Eq. (11), one has to find the integrand $(1/V) \cdot (dW/dz)$ and express it as a function of z. If it were possible to find a z plane where a function P_z of z were known, then due to Eq. (5), dW/dz would be known as a function of z. If, furthermore, one can find the conformal mapping that maps the region R_z in the z plane onto the region R_V (the distribution of complex velocities), then according to Eq. (7), the relation $V = G_V(z)$ will be well defined. As a consequence, the integral (11) can be rewritten as

$$Z_f = f(z_f) = \int_{z_0}^{z_f} \frac{1}{G_V(z)} \cdot \frac{dP_z(z)}{dz} dz \qquad (12)$$

and it will be possible to determine it for any point z_f. In particular, if the point z_f lies on the contour of R_z, one will be able to determine a Z_f that will be a point of the boundary of the airfoil the designer wants to design.

In any problem of inverse design, the choice of the z plane is fundamental. In the case of design of a single airfoil, the most convenient z plane is the one that has a circular obstacle centered at the origin. This z plane will be the one used in the method presented in this article. Observe that this plane has the advantage that the general expressions for W and dW/dz as a function of z [Eqs. (8) and (9)] are known, and so $dP_z(z)/dz$ is completely determined. Then, since the velocity contour has been specified, one has to find the conformal mapping $G_V(z)$ that maps R_z onto R_V. How to do this will be explained in a following section.

Explicit Integrals for the Calculus of the Airfoil

With the choice of z plane as the plane of the circular obstacle, one can replace Eq. (9) into the integral (12)

$$Z_f = \int_{z_0}^{z_f} \frac{1}{G_V(z)} \left[q_0 e^{-i\alpha} - q_0 e^{i\alpha} R^2 \frac{1}{z^2} + \frac{\Gamma}{2\pi i} \frac{1}{z} \right] dz \tag{13}$$

The contour of the circular obstacle in the z plane corresponds to the contour of the airfoil in the physical Z plane, then, choosing the point z_f as a point of the surface of the circular obstacle

$$z_f = Re^{i\phi_f}$$

and calculating Eq. (13), one will have found a point Z_f of the airfoil that has velocity $V_f = G_V(z_f)$. If the point z_0 is also chosen on the contour, i.e.,

$$z_0 = Re^{i\phi_0}$$

the point $Z = 0$ (origin of the physical Z plane) will correspond to another point of the airfoil.

Particularizing and integrating Eq. (13) along the circular obstacle

$$z = Re^{i\phi}$$

$$dz = iRe^{i\phi}\, d\phi$$

and thus,

$$Z_f = g(\phi_f)\text{eq} = \int_{\phi_0}^{\phi_f} \frac{1}{G_V(z)} \left[q_0 2i \sin(\phi - \alpha) + \frac{\Gamma}{2\pi i} \frac{1}{R} \right] iR\, d\phi \tag{14}$$

The complex integral has been reduced to a simpler angular integral. Also, the following parameters have appeared $\{\alpha, q_0, \Gamma, R\}$. There are more hidden parameters in the term $G_V(z)$. All of them cannot take arbitrary values and have to be adjusted in order to meet dynamic and geometric constraints.

Condition of Incidence at Infinity ($Z \to \infty$)

The solution is simplified if one imposes that the movement produced by the uniform stream be the same far away from the obstacles for both the airfoil in the Z plane and the circular obstacle in the z plane. To achieve this one imposes the following conditions:

$$Z = \lim_{z \to \infty} f(z) = z \quad \text{or equivalently} \quad z = \lim_{Z \to \infty} f^{-1}(Z) = Z \tag{15}$$

Then, using Eq. (15), one obtains that the complex velocity of the incident uniform stream $V_\infty = q_\infty e^{-i\theta_\infty}$ satisfies

$$q_\infty e^{-i\theta_\infty} = q_0 e^{-i\alpha}$$

or equivalently

$$q_\infty = q_0, \qquad \theta_\infty = \alpha \tag{16}$$

Conditions Due to Stagnation Points

The points S (forward stagnation or impact point) and T (trailing edge) will correspond to two other points z_S and z_T:

$$z_S = Re^{i(\pi - b)}, \qquad z_T = Re^{i\phi_T} \tag{17}$$

on the circular obstacle ($z = Re^{i\phi}$) in the z plane. These points have to satisfy the condition $dW/dz = 0$, i.e.,

$$\left[q_0 e^{-i\alpha} - q_0 e^{i\alpha} R^2 \frac{1}{z^2} + \frac{\Gamma}{2\pi i} \frac{1}{z} \right]_{z = Re^{i\phi}} = 0 \tag{18}$$

Using Eqs. (17) and (18), one gets

$$2i \sin(b + \alpha) = -\frac{\Gamma}{2\pi i} \cdot \frac{1}{Rq_0} \tag{19}$$

$$\phi_T = b + 2\alpha \tag{20}$$

$$z_T = Re^{i(b + 2\alpha)} \tag{21}$$

There are two more constraints that come from the correspondence between each point V in the hodograph and its correspondent point in the z plane:

$$V = G_V(z)$$

In particular, the point $V_S = 0$ corresponding to S has to be related to z_S, and the point V_T corresponding to the complex velocity of the flow at T has to be related to z_T, and so one has

$$0 = V_S = G_V(z_S), \qquad q_T e^{-i\theta_T} = V_T = G_V(z_T) \tag{22}$$

Closure Condition

This condition is essential since a physically meaningful airfoil corresponds to a closed contour. The general equation of closure for the contour (G.E.C.C.) imposes conditions on the different parameters to achieve a closed airfoil. Without this condition all efforts would be useless. The G.E.C.C. is surprisingly simple and generally applicable.

The G.E.C.C. is deduced from the condition that the value of the integral (11), calculated over the closed contour associated to the airfoil has to be zero:

$$0 = \Delta Z = \oint_c \frac{1}{V} \frac{dW}{dz}\, dz$$

In a similar way as done in Ref. 8 and using Eq. (16), it is possible to demonstrate the following:

Theorem 1: The single necessary and sufficient condition, to be satisfied by the parameters of design of an airfoil in an inverse method in order to obtain a closed airfoil is

$$\frac{\Gamma}{2\pi i} = -\left[\frac{dV}{dz} \cdot z^2 \right]_{z \to \infty} \tag{23}$$

Restriction to Prescribed VCs and Some Considerations

The VC comes from the obstacle(s) or simple closed contour(s) that defines the boundary of R_Z. This, together with the fact that its defining function dP/dZ is an analytic function, may lead one to believe that the VC will necessarily be a simple closed contour defining the boundary of R_V. However, there are cases where the VC self-intersects or forms a loop. In Fig. 4 an example of this kind of VC is shown. When this

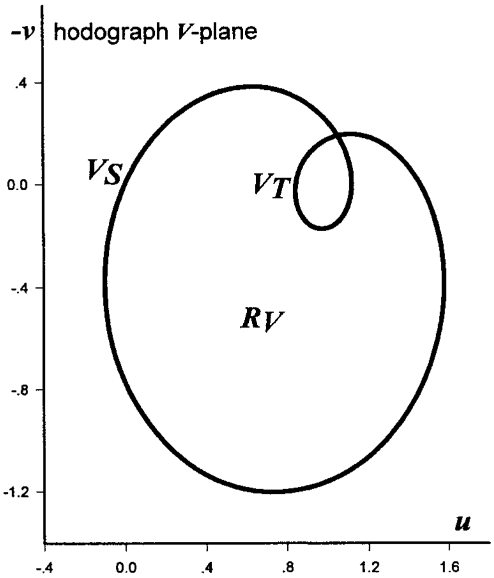

Fig. 4 Example of a velocity contour for a symmetrical airfoil at a moderate direction of incidence.

happens, the mapping of the domain R_z onto R_V by the analytic function G_V is not one-to-one. The inverse of G_V does not exist and herein lies the difficulty of this case.

The problem for a self-intersecting VC has been solved, but this difficulty obviously needs a special treatment, and so the present paper is restricted to the cases of non-self-intersecting (without loops) VCs. This restriction forbids the inclusion of some interesting cases, but because all the VCs formed by simple closed nonintersecting contours of arbitrary shapes are permitted, one still has a number of equally interesting possibilities included. Some examples will be given in a final section.

The method allows the designer to obtain a geometric shape, a direction of incidence θ_∞, and the speed q_∞ of the uniform stream, in such a way that if the airfoil is submitted to a stream with these characteristics, the complex velocity along the airfoil coincides with the input VC. As a consequence, the airfoil under these conditions will satisfy all the imposed requirements.

As presented here, the method has the advantage that there are no restrictions for the speed q_T of the trailing edge, which is of importance for the problem of boundary-layer control and for the lift produced by the upper surface. However, the fact that one cannot specify the speed q_∞ may disturb some designers. The designer can obtain an estimation of the value of q_∞ using the fact that for an airfoil of high lift with good performance and with zero trailing-edge angle the value of q_∞ usually lies between 1.05–1.35 of the value of q_T. If this is not enough, there are two other alternatives:

1) A variant of the method permits the designer to impose a definite q_∞ for the stream and then only the relative speeds $q_{\rm rel} = q_P/q_{P1}$, in all the points P of the airfoil, with respect to a reference point with speed q_{P1} on the airfoil. This reference speed is a free parameter and is determined a posteriori by the method.

2) Modifying on the VC the position of the point V_T until an acceptable q_∞ is obtained. The latter usually works well and is also effective for the problem of obtaining a specified C_L.

Conformal Mapping $V = G_V(z)$

Assuming that the designer has defined the VC in the hodograph that gives the complex velocities on the surface of the airfoil, the problem of looking for the map G_V

$$z \xrightarrow{G_V} V$$

that maps the contour of the circular obstacle into the VC and the region R_z exterior to the circular obstacle onto R_V arises.

As expressed in the last section, it is also assumed that one has a completely arbitrary prescribed VC with the unique condition that it does not have loops. All the VCs that consist of simple (nonintersecting) closed curves are, in principle, allowed.

Remembering from Eqs. (6) and (7) that G_V is an analytic function and it maps a simple closed curve (the contour of the circular obstacle) on another simple closed curve (the VC). It is possible to deduce that the expression

$$G_V(z) = V \tag{24}$$

maps the region R_z one-to-one and onto the region R_V. Then, the inverse

$$G_V^{-1}(V) = z \tag{25}$$

which transforms the distribution of complex velocities R_V onto the exterior of the circular obstacle is well defined.

The conformal maps G_V are not unique. They depend on two parameters (these are the hidden parameters that were mentioned earlier). First, G_V depends on a parameter that specifies in which point z_S of the circular obstacle the point $V = 0$ is mapped into. Evidently, according to Eq. (17), this parameter is b, and so $G_V(z)$ should depend on b. Second, one has to specify the behavior of the conformal mapping infinitely far away from the circular obstacle, i.e.,

$$\lim_{z\to\infty} V = V_\infty$$

then, the other parameter must be the complex velocity of design corresponding to the incident stream $V_\infty = q_\infty e^{-i\theta_\infty}$. It will be helpful to rewrite Eqs. (24) and (25) as

$$G_V(z, b, V_\infty) = V \quad \text{and} \quad G_V^{-1}(V, b, V_\infty) = z \tag{26}$$

to take into account explicitly this dependence on the unknown parameters b and V_∞.

Now one has to address the fundamental problem of obtaining an explicit expression for G_V. In what follows a method is described that the author considers the most simple, general, and effective. It has been developed theoretically and computationally on the basis of successive transformations. One proceeds by the following steps:

1) This step is necessary only if the VC has a breaking point (or corner) $V_{\rm bp}$, i.e., a nonconformal point where the tangent to the contour changes abruptly. The first step consists of a linear fractional transform

$$L_0(w) = (aw + b)/(cw + d) \tag{27}$$

to map the point $V_{\rm bp}$ to the origin and the contour into the angular sector. Then one applies the function L_1

$$L_1(w) = w^{\pi/\alpha_{\rm bp}} \tag{28}$$

(where $\alpha_{\rm bp}$ is the interior angle of breaking) in order to remove the breaking point. These procedures must be repeated successively if there are more corners. The mapping

$$\xi_1 = L_1[L_0(V)] \tag{29}$$

defines a region $R_{\xi 1}$ with a smooth boundary and connected one-to-one to R_V. In particular, for any choice of the point V_∞, one has a well-defined point $\xi_{1\infty}$.

2) In this second step, one finds the transformation that maps $R_{\xi 1}$ onto the interior (or equivalently exterior) of a circular disc U. This is done, in principle, with a technique

called RL mapping (RLM), based on the Riemann mapping theorem that constructs a sequence $\{H_N\}$ of explicit transformations such that $\lim_{N\to\infty} H_N$ has the required property. Although one can map $R_{\xi 1}$ onto a practically circular disc by choosing N sufficiently large, it is not true that the inverse H_N^{-1} maps the perfect circular disc onto a region that is practically equal to $R_{\xi 1}$. The combination of the RLM with the Theodorsen–Garrick method (TGM) allows us to circumvent this problem. The idea consists of using the RLM to get a good approximation to the circular disc, and then to use the TGM to map this approximation exactly onto U. All this is made explicit in the following two substeps:

RLM

Transform the region $R_{\xi 1}$ onto a quasicircular obstacle of radius approximately equal to 1. To do this one proceeds as follows:

Define the analytic function

$$H_0(\xi_1) = (\xi_1 - \xi_{1\infty})/\lambda \quad \text{with} \quad \lambda > \max\{|\xi_1 - \xi_{1\infty}|/\xi_1 \in R_{\xi 1}\} \tag{30}$$

It follows that $H_0(R_{\xi 1}) \subset U$ and

$$H_0(\xi_{1\infty}) = 0 \tag{31}$$

Having defined the domain $H_0(R_{\xi 1})$, let $x_0 = |x_0|e^{i\nu_0} = d_0 e^{i\nu_0}$ be the point of the boundary of $H_0(R_{\xi 1})$ nearest to the origin, and such that the half-line from the origin through x_0 intersects the said boundary only at x_0. If this condition is not met, one can apply a fractional linear transformation and a square root (with the branch cut out of the region $R_{\xi 1}$) to modify the boundary in order to meet the condition. Take γ_0 as a negative real such that $|x_0| < |\gamma_0| < 1$ and γ_0 is as near as possible to $-|x_0|$. Then denoting the complex number $e^{-i(\pi+\nu_0)}$ by c_{ν_0}, one defines the analytic function

$$H_1(\xi_1) = F_0^{-1} \circ c_{\nu_0} H_0(\xi_1) \tag{32}$$

where here and in the following, the symbol '$\circ$' is used to express the composition of functions, i.e., $h \circ g(w) = h(g(w))$ and F_0^{-1} is the inverse of

$$F_0(w) = \frac{[(w + \beta_0)/(1 + w\overline{\beta_0})]^2 + \gamma_0}{1 + \overline{\gamma_0}[(w + \beta_0)/(1 + w\overline{\beta_0})]^2} \tag{33}$$

with

$$\beta_0 = \sqrt{-\gamma_0} \tag{34}$$

Observe that

$$H_1(\xi_{1\infty}) = 0 \tag{35}$$

Now, one proceeds with the well-defined domain $H_1(R_{\xi 1})$ as done with the domain $H_0(R_{\xi 1})$, and so proceeds iteratively by finding $H_2(R_{\xi 1})$ from $H_1(R_{\xi 1})$, $H_3(R_{\xi 1})$ from $H_2(R_{\xi 1})$, etc. Then in the nth step

$$H_n(\xi_1) = F_{n-1}^{-1}[c_{\nu_{n-1}} H_{n-1}(\xi_1)] \tag{36}$$

From the Riemann mapping theorem (e.g., see Ref. 9)

$$\lim_{N\to\infty} H_N(R_{\xi 1}) = U \tag{37}$$

As a consequence, choosing N sufficiently large, $H_N(R_{\xi 1})$ will be a quasicircular region with a radius a little smaller than one here denoted $R_{\xi 2}$. Then according to Eq. (36):

$$\xi_2 = H_N(\xi_1) = F_{N-1}^{-1} \circ c_{\nu_{N-1}} F_{N-2}^{-1} \circ c_{\nu_{N-2}} F_{N-3}^{-1} \circ \cdots \circ c_{\nu_1} F_0^{-1} \circ c_{\nu_0} H_0(\xi_1) \tag{38}$$

One can write

$$\xi_2 = L_2(\xi_1) \quad \text{and} \quad \xi_1 = L_2^{-1}(\xi_2) \tag{39}$$

with

$$L_2 \equiv F_{N-1}^{-1} \circ c_{\nu_{N-1}} F_{N-2}^{-1} \circ \cdots \circ c_{\nu_2} F_1^{-1} \circ c_{\nu_1} F_0^{-1} \circ c_{\nu_0} H_0 \tag{40}$$

$$L_2^{-1} \equiv H_0^{-1} \circ \overline{c_{\nu_0}} F_0 \circ \overline{c_{\nu_1}} F_1 \circ \overline{c_{\nu_2}} F_2 \circ \cdots \circ \overline{c_{\nu_{N-2}}} F_{N-2} \circ \overline{c_{\nu_{N-1}}} F_{N-1} \tag{41}$$

where

$$F_{n-1}(w) = \frac{[(w + \beta_{n-1})/(1 + w\overline{\beta_{n-1}})]^2 + \gamma_{n-1}}{1 + \overline{\gamma_{n-1}}[(w + \beta_{n-1})/(1 + w\overline{\beta_{n-1}})]^2} \tag{42}$$

$$c_{\nu_n} = e^{-i(\pi+\nu_n)} \tag{43}$$

with

$$x_n = d_n e^{i\nu_n} \tag{44}$$

where x_n is the point of the boundary of the region $H_n(R_{\xi 1})$, which is nearest to the origin. Equations (40) and (41) define completely the analytic function L_2 and its inverse that can be explicitly obtained if one proceeds iteratively determining the set of complex constants $\{\lambda, \nu_n, \gamma_n, \beta_n\}$.

The explicit expression

$$\xi_2 = L_2\{L_1[L_0(V)]\} = G_1^{-1}(V, V_\infty) \tag{45}$$

allows one to transform the VC into a quasicircular contour and V_∞ into the origin of the ξ_2 plane. The inverse transformation is

$$V = L_0^{-1}\{L_1^{-1}[L_2^{-1}(\xi_2)]\} = G_1(\xi_2, V_\infty) \tag{46}$$

In the right-hand side (RHS) of Eqs. (45) and (46) the dependence on the parameter V_∞ has been made explicit. The number N of iterations required for L_2 varies with the shape of the VC. One can estimate the degree of convergence as follows; remembering the definition of d_n, one can expect

$$d_n \approx \sqrt{d_{n-1}} = (d_{n-1})^{1/2}$$

That is to say

$$d_n \approx (d_0)^{1/2n}$$

As a numerical example, let us suppose that $d_0 = 0.4$. For $n = 10$, one gets $d_{10} = (0.4)^{1/20} = 0.95$, so that after 10 iterations one can expect an approximation of 90% on that sector.

TGM

Once the map $G_1(\xi_2, V_\infty)$ and the quasicircular contour are fixed, one has to find another conformal mapping G_2:

$$\xi_3 \xrightarrow{G_2} \xi_2$$

$$G_2(\xi_3) = \xi_2 \quad \text{or} \quad G_2^{-1}(\xi_2) = \xi_3 \tag{47}$$

which maps the region $R_{\xi 2}$ in the ξ_2 plane onto the region $R_{\xi 3}$ interior to a circular obstacle in a ξ_3 plane. First of all, it is possible to deduce that the general transformation doing this has to have the form

$$\xi_2 = G_2(\xi_3) = \xi_3 \exp\left\{\sum_{n=0}^{\infty} (A_n + iB_n)\xi_3^n\right\} \tag{48}$$

and then its derivative is

$$\frac{d\xi_2}{d\xi_3} = \exp\left\{\sum_{n=0}^{\infty}(A_n + iB_n)\xi_3^n\right\}\left[1 + \sum_{n=0}^{\infty} n(A_n + iB_n)\xi_3^n\right] \tag{49}$$

To determine the coefficients A_n and B_n, one applies the complex logarithm $\mathcal{Ln}$ to both members of Eq. (48), and obtains

$$\mathcal{Ln}\left[\frac{\xi_2}{\xi_3}\right] = \sum_{n=0}^{\infty}(A_n + iB_n)\xi_3^n$$

For points ξ_3 and ξ_2 belonging to their respective contours, one can write ξ_3 as $\xi_3 = R_3e^{i\phi_3}$ and ξ_2 as $\xi_2 = \tau e^{i\omega}$, replacing this in the latter equation, one gets:

$$\mathcal{Ln}\left[\frac{\tau e^{i\omega}}{R_3e^{i\phi_3}}\right] = \sum_{n=0}^{\infty}(A_n + iB_n)R_3^n e^{in\phi_3} \tag{50}$$

One knows τ as a function of ω, i.e., one has defined $\tau = \tau(\omega)$, R_3 is a constant (equal to 1). One gets a first approximation putting $\omega = \omega^{(1)}(\phi_3)$, and then, $\tau = \tau^{(1)}[\omega^{(1)}(\phi_3)]$. This permits us to use the fast Fourier transform (FFT) algorithm iteratively directly on the series (50) by taking $N + 1$, discrete equally spaced values of ϕ_3. Once the coefficients A_n and B_n have been determined, one has the explicit function G_2.

Then, by means of the function $\xi_4 = G_3^{-1}(\xi_3) = R/\xi_3$, one connects the interior of the disc R_{ξ_3} with the region R_{ξ_4} exterior to the circular obstacle in the ξ_4 plane. One can write

$$\begin{aligned} G_4(\xi_4, V_\infty) &= V \\ G_4^{-1}(V, V_\infty) &= \xi_4 = Re^{i\phi_4} \end{aligned} \tag{51}$$

where $G_4 = G_1 \circ G_2 \circ G_3$. One can avoid repeating these steps for each V_∞ by means of an appropriate linear fractional transform added to G_4.

3) Assuming without loss of generality that the complex velocity $V_S = 0$ of the forward stagnation point S corresponds to the point $\xi_4 = \xi_{4S} = -R$, a simple rotation moves this point to satisfy Eq. (18). And one gets the expression for G_V:

$$\begin{aligned} G_4(e^{ib}z, V_\infty) &= G_V(z, b, V_\infty) = V \\ e^{-ib}G_4^{-1}(V, V_\infty) &= G_V^{-1}(V, b, V_\infty) = z \end{aligned} \tag{52}$$

Having this well-defined $G_V(z, b, V_\infty)$, one can do the rest of the calculation.

System of Equations

Recall the results obtained up to now:

$$Z_f = \int_{\phi_0}^{\phi_f}\frac{1}{G_V(z)}\left[i2q_0\sin(\phi - \alpha) + \frac{\Gamma}{2\pi i}\frac{1}{R}\right]iR\,d\phi \tag{53}$$

$$q_\infty = q_0 \tag{54}$$

$$\theta_\infty = \alpha \tag{55}$$

$$2i\sin(b + \alpha) = -\frac{\Gamma}{2\pi i}\cdot\frac{1}{Rq_0} \tag{56}$$

$$z_T = Re^{i(b+2\alpha)} \tag{57}$$

$$z_S = Re^{i(\pi - b)} \tag{58}$$

Furthermore, for $V_S = 0$ of S and $V_T = q_Te^{-i\theta_T}$ at T of the airfoil, one has

$$G_V^{-1}(0, b, V_\infty) = z_S = Re^{i(\pi-b)} \tag{59}$$

$$G_V^{-1}(V_T, b, V_\infty) = z_T = Re^{i(b+2\alpha)} \tag{60}$$

The transformation G_V defines a value for R. Nevertheless, whatever the value of R, it simply acts as a scaling factor of the size of the airfoil. It can be chosen to be 1. Finally, the condition for a closed contour (23) can be written as

$$\frac{\Gamma}{2\pi i} = -\left[\frac{dG_V(z, b, V_\infty)}{dz}\cdot z^2\right]_{z\to\infty} \tag{61}$$

To calculate the airfoil by means of the integral (53), one has to find all the unknown parameters: V_∞, b, α, Γ, and q_0. To do this the system of Eqs. (54–61) has to be used as will be discussed in the next section.

Determination of V_∞, b, α, Γ, and q_0

Equating Eqs. (56) and (61), one has

$$2iRq_0\sin(b + \alpha) = \left[\frac{dG_V(z, b, V_\infty)}{dz}\cdot z^2\right]_{z\to\infty} \tag{62}$$

From Eqs. (59) and (60) one gets

$$\begin{aligned} G_V^{-1}(V_T, b, V_\infty)\overline{G_V^{-1}(0, b, V_\infty)} &= Re^{-i(\pi-b)}Re^{i(b+2\alpha)} \\ &= -R^2e^{i2(b+\alpha)} \end{aligned} \tag{63}$$

One can rewrite (63) as

$$G_4^{-1}(V_T, V_\infty)\overline{G_4^{-1}(0, V_\infty)} = -R^2e^{i2(b+\alpha)} \tag{64}$$

using the second equation of Eqs. (52) and (62) as

$$2iRq_0\sin(b + \alpha) = \left[\frac{dG_4(e^{ib}z, V_\infty)}{dz}\cdot z^2\right]_{z\to\infty} \tag{65}$$

using the first equation of Eq. (52). The change of variables $e^{ib}z = \xi_4$ gives

$$2iRq_0\sin(b + \alpha) = \left[e^{-ib}\cdot\frac{dG_4(\xi_4, V_\infty)}{d\xi_4}\cdot\xi_4^2\right]_{\xi_4\to\infty} \tag{66}$$

Using Eqs. (59) and (60), (64), and (66) can be rewritten as

$$G_4^{-1}(V_T, V_\infty)\overline{G_4^{-1}(0, V_\infty)} = -R^2e^{i2(b+\theta_\infty)} \tag{67}$$

$$2iRq_\infty\sin(b + \theta_\infty)e^{ib} = \left[\frac{dG_4(\xi_4, V_\infty)}{d\xi_4}\cdot\xi_4^2\right]_{\xi_4\to\infty} \tag{68}$$

Taking the argument of the complex numbers in both members of Eq. (67), one gets

$$\frac{1}{2}\arg[-R^{-2}G_4^{-1}(V_T, V_\infty)\overline{G_4^{-1}(0, V_\infty)}] = b + \theta_\infty \tag{69}$$

Therefore, b can be considered a function of V_∞:

$$b = B_b(V_\infty) = \tfrac{1}{2}\arg[-R^{-2}G_4^{-1}(V_T, V_\infty)\overline{G_4^{-1}(0, V_\infty)}] - \theta_\infty \tag{70}$$

Inserting Eq. (70) into Eq. (68), one obtains

$$2iRq_\infty\sin[B_b(V_\infty) + \theta_\infty]e^{iB_b(V_\infty)} = \left[\frac{dG_4(\xi_4, V_\infty)}{d\xi_4}\cdot\xi_4^2\right]_{\xi_4\to\infty} \tag{71}$$

Equation (71) is a simple complex equation with one complex unknown: V_∞. This can be solved to determine the correct value of V_∞ (or equivalently q_∞ and θ_∞). Then b is obtained from Eq. (70). Finally, q_0, α, and Γ are obtained from Eqs. (54), (55), and (56), respectively.

Replacing Eq. (56) into Eq. (53), one has

$$Z(\phi_f) = -q_0 R 2 \int_{\phi_0}^{\phi_f} \frac{1}{G_V(z, b, V_\infty)} \times [\sin(\phi - \alpha) - \sin(b + \alpha)]\, d\phi \tag{72}$$

Once the parameters have been calculated this expression permits the determination of the airfoil.

As a consequence, the problem of finding a closed airfoil from any VC has been reduced and decoupled. Thus, if such an airfoil exists, then there has to be a complex number V_∞ that is the solution of Eq. (71). Furthermore, it follows that this $V_\infty = q_\infty e^{-i\theta_\infty}$ is exactly the velocity of design, and the airfoil will satisfy all the requirements prescribed through the VC under these conditions. Finally, the determination of the airfoil itself is reduced to a real integration of a simple, complex, and well-defined integrand.

Determination of the Pressure Distribution

Each point Z_f of the airfoil was determined by the value of an angle ϕ_f, and as a consequence is associated to a point $z_f = Re^{i\phi_f}$ on the circle of the plane z. To determine the distribution of velocities over the designed airfoil (whose geometry is now known) as a function of the angle α_z of the incident stream, one uses

$$V = \frac{dW}{dZ}$$

In particular, for a point Z_f of the airfoil and its corresponding $z_f = Re^{i\phi_f}$, it is possible to deduce that

$$V_f = [-2q_0 R][\sin(\phi_f - \alpha_Z) - \sin(b + \alpha_Z)] \left[\frac{d\phi(\phi_f)}{dZ}\right] \tag{73}$$

This expression allows one to determine the velocity (and the pressure) over each point of the airfoil for given angle of incidence α_Z for ideal flow conditions.

Tested Examples

The method is tested by redesigning two well-known airfoils. The VCs are calculated from the tabulated coordinates by a direct panelization method for some chosen complex incidence velocity $V_l = q_l e^{-i\theta_l}$. These VCs are used as input for the present method and the resulting airfoils are compared with the original airfoils.

Example 1: Redesign of the E 201 Airfoil

The E 201 is a well-known airfoil designed by Eppler, its coordinates were taken from Ref. 10. The VC corresponding to an incidence $V_l = q_l e^{-i\theta_l}$, where $q_l = 1$ and $\theta_l = 10$ deg was determined by a panelization method. Since one is seeking to reobtain the E 201 via the inverse method, it is necessary to calculate the VC with accuracy, and so it is recommended to determine the VC using as many airfoil coordinate points as possible (e.g., 250–300). If this amount of points is unavailable, a spline interpolation method can be used to generate more airfoil points. Doing this is not the same as interpolating on a VC obtained with few airfoil points. The latter should not be done. For the E 201, 33 original airfoil points were taken and around 280 were generated by splines. For points very near to the trailing edge of the E 201 the exact determination of the VC is difficult, and so no information was input on a very small trailing-edge zone (less than 2% of the chord). The VC generated is shown in Fig. 5, it is non-self-intersecting and so it can be used as an input VC.

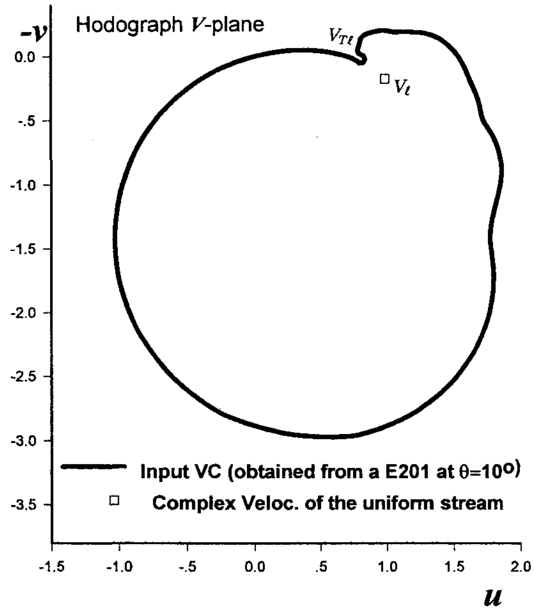

Fig. 5 Velocity contour for a E 201 airfoil, $q_l = 1$ and $\theta_l = 10$ deg.

Because of this trailing-edge problem, one did not exactly know the correct value of the complex velocity V_{Tt} of the E 201's trailing edge; an estimated value for V_T was chosen. The analytic function G_V was determined following the steps described before. Finally, Eq. (71) was used to find the value of V_∞. Then, a new point on the VC for V_T was re-entered and the process repeated until a value V_∞ concordant with V_l was obtained. Here, the process was stopped when the values $q_\infty = 1.0007$ and $\theta_\infty = 10.011$ deg were obtained. They correspond to $V_T = 0.7852 + i0.0918$.

The determination of G_V was done by the following procedure:

1) The VC did not present corners.

2) The mappings L_0 and L_1 were only used as a simple translation of the origin into the point $w_g = 0.8 - i0.02$ and as a square root with its branch cut forming an angle of 120 deg.

3) Then, to map the contour into a quasicircular contour the RLM process was used, applying 200 RLM iterations. Figure 6 shows successive steps of the process, it is surprising how well the RLM technique works.

4) The TGM was applied using 256 coefficients. Finally, the remaining steps were done and the analytic function G_V was obtained. Equation (71) finds the previous value of V_∞ and Eqs. (70), (54), (55), and (56) determine all the unknown parameters b, q_0, α, and Γ. Then, output airfoil A was designed using Eq. (72).

The values given for q_∞ and θ_∞, corresponding to airfoil A when the procedure was stopped, differ from q_l and θ_l used for the calculation of the VC of the E 201 by about 0.1%. Then, if the method works well, airfoil A should be equal to the E 201. The likeness between these two airfoils can be appreciated in Fig. 7 (where the normalized airfoils are shown by increasing the scales in the ordinates). The discrepancy is less than 0.03% of the chord length or less than 0.3% of the profile width. Airfoils B and C of Fig. 7 are other airfoils designed using exactly the same input VC and varying only with V_T. For airfoil B, $V_T = 0.9176 + i0.1943$ and the resulting design velocity V_∞ was $q_\infty = 1.0331$, $\theta_\infty = 8.1989$ deg. For airfoil C, $V_T = 0.8323 - i0.0093$ and the resulting design velocity V_∞ was $q_\infty = 0.9602$ and $\theta_\infty = 11.3947$ deg. Although A, B, and C airfoils and obviously the E 201 airfoil generate the same VC for their respective design velocities V_∞ (as was verified by a direct panelization method), airfoils B and C

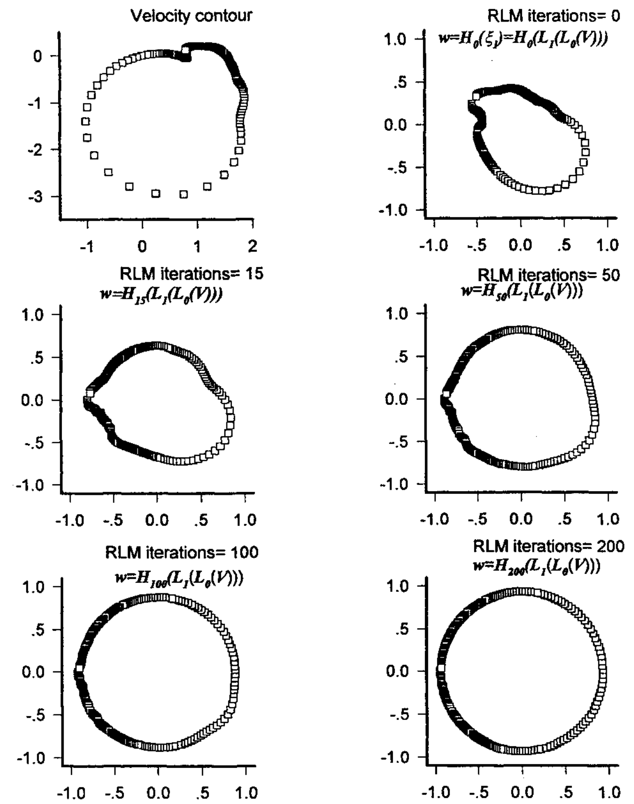

Fig. 6 Successive mapping of the E 201 airfoil's velocity contour into a quasicircular contour.

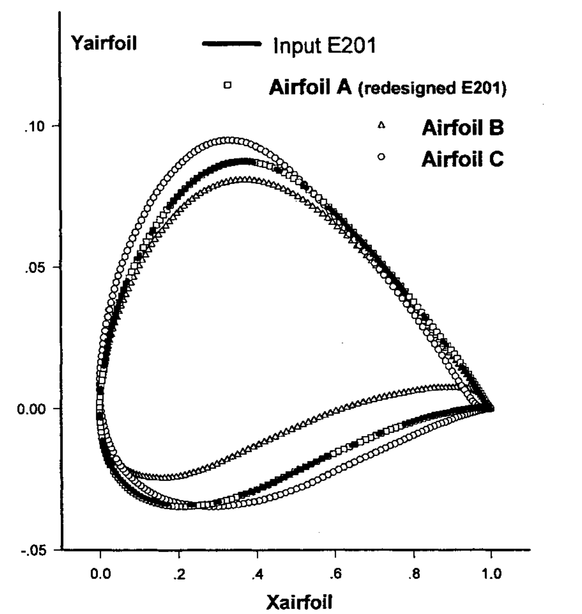

Fig. 7 E 201 airfoil, the E 201 airfoil's redesign, and two other airfoils designed using the velocity contour of the E 201.

differ in their C_p distribution as shown in Fig. 8 (for values of $-C_p \leq 5$).

Example 2: Redesign of the RAE 101-06-30-65 Airfoil

The RAE 101-06-30-65 is another well-known airfoil, its coordinates can be found in Ref. 11 and it was chosen as the second test case. The VC was determined by a panelization method corresponding to an incidence $V_l = q_l e^{-i\theta_l}$, where $q_l = 1$ and $\theta_l = 3.27$ deg. The latter value was chosen because it is the ideal incidence value, which together with the Mach number of 0.65 are the dynamical conditions for its ideal

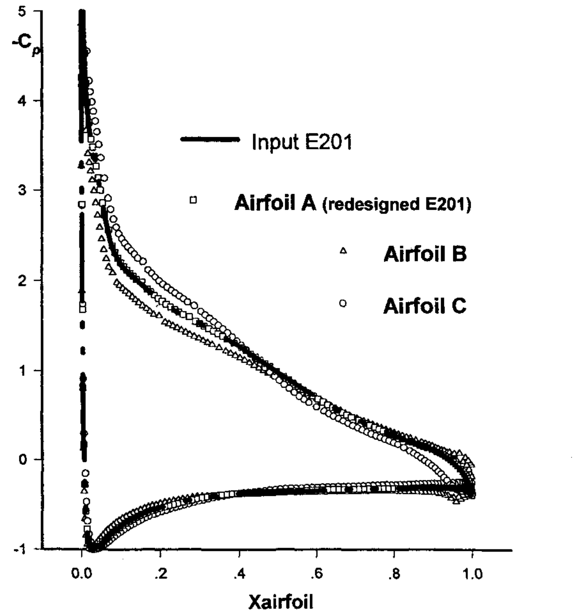

Fig. 8 Pressure distributions of the airfoils shown in Fig. 7.

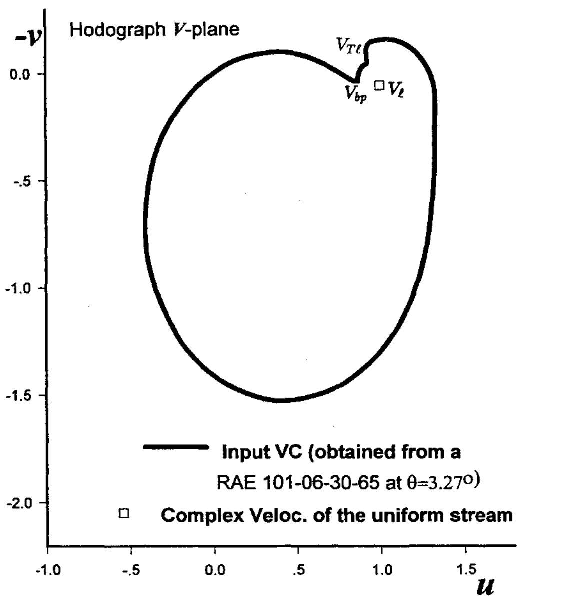

Fig. 9 Velocity contour for a RAE 101-06-30-65 airfoil, $q_l = 1$ and $\theta_l = 3.27$ deg.

behavior. The Mach condition will not be used, since here the flow is considered as incompressible. To calculate an exact VC, the recommendations given for example 1 are general and were also applied here. To do this example, 33 original airfoil points were taken from Ref. 11 and around 280 were generated by splines. The small zone of the VC corresponding to the trailing-edge zone was left to be naturally defined by the method. The VC generated is shown in Fig. 9, it is a non-self-intersecting VC, and so it can be used as an input VC.

Again, the complex velocity V_{Tl} corresponding to the RAE 101-06-30-65's trailing edge was not known exactly. An estimated value for V_T was chosen. The analytic function G_V was determined following the steps described above. Finally, Eq. (71) was used to find the value of V_∞. Then, a new point on the VC for V_T was re-entered and the process repeated until a value V_∞ concordant with V_l was obtained. Here, the process was stopped when the values $q_\infty = 1.0019$ and $\theta_\infty = 3.2699$ deg were obtained. They corresponded to a $V_T = 0.9232 + i0.0693$.

The determination of G_V was done by the following procedure:

1) It was found that the VC presented a corner, therefore the mappings L_0 and L_1 had to be applied. The breaking point V_{bp} was determined to be at $0.8695 - i0.0379$. L_0 was reduced to a simple translation and the angle of breaking was estimated to be $\alpha_{bp} = 2\pi$. The corresponding branch cut angle of the root defined by L_1 was estimated to be equal to 129.1568 deg.

2) The RLM process was directly used to map the contour into a quasicircular one, applying 200 RLM iterations. Figure 10 shows successive steps of the process, and again, it can be seen how well the RLM technique works.

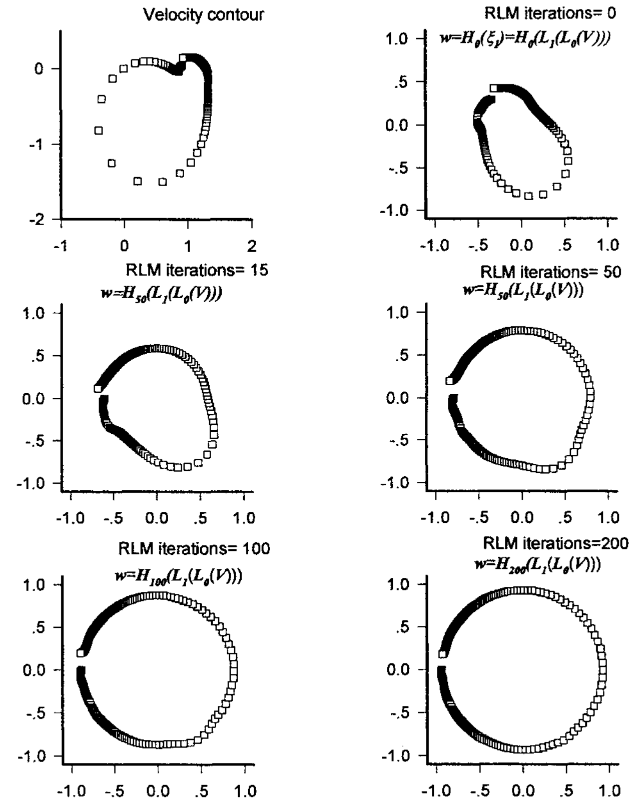

Fig. 10 Successive mapping of the RAE 101-06-30-65 airfoil's velocity contour into a quasicircular contour.

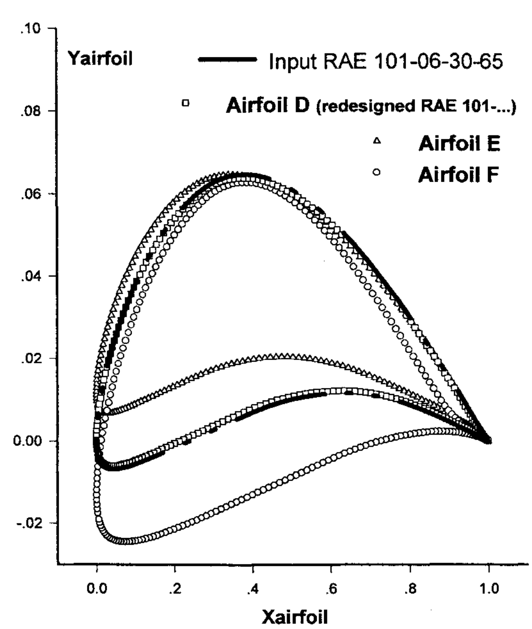

Fig. 11 RAE 101-06-30-65 airfoil, the RAE 101 airfoil's redesign, and two other airfoils designed using the velocity contour of the RAE 101-06-30-65.

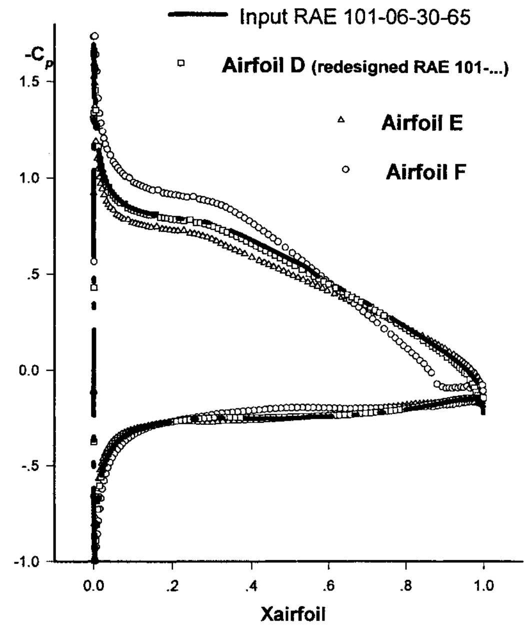

Fig. 12 Pressure distributions of the airfoils shown in Fig. 11.

3) The TGM was applied using 256 coefficients. Finally, the remainder steps were done and the explicit expression of G_V was obtained. Using Eq. (71) to find the previous value of V_∞ and Eqs. (70), (54), (55), and (56) to determine all the unknown parameters b, q_0, α, and Γ. Then, output airfoil D was designed using Eq. (72).

The values of q_∞ and θ_∞ differ in less than 0.2% from those of q_l and θ_l used for the calculation of the VC of the RAE 101. The likeness between airfoil D and RAE 101 can be appreciated in Fig. 11. A small discrepancy (less than 0.09% of the chord length and less than 2% of the width) can be detected between the two airfoils, it may be due to a small difference between the true angle of breaking α_{bp} and its input value 2π; α_{bp} may be a little smaller. Airfoils E and F are other airfoils designed using exactly the same input VC and varying only by V_T. For airfoil E, $V_T = 0.9229 + i0.1228$ and the resulting design velocity V_∞ was $q_\infty = 1.0158$, $\theta_\infty = 2.2085$ deg. For airfoil F, $V_T = 0.9174 + i0.0419$ and the resulting design velocity V_∞ was $q_\infty = 0.9708$, $\theta_\infty = 4.9699$ deg. Although airfoils D, E, F, and obviously the RAE 101 airfoil generate the same VC for their respective design velocities V_∞ (as was verified by a direct panelization method), airfoils E and F differ in their C_p distribution as shown in Fig. 12.

Conclusions

An exact solution of an inverse method has been presented, giving the procedure to determine the airfoil satisfying all requirements imposed via any non-self-intersecting VC. The method returns as output of the geometry of the airfoil and a corresponding freestream velocity such that the airfoil subjected to these conditions generates exactly the required VC.

The presented examples intend to illustrate the method, and show its usefulness in the design of airfoils.

The case of self-intersecting VC has also been solved, thus obtaining a completely general method for arbitrary VCs. This will be the content of a future contribution.

The method presented admits extensions to cover the case of compressible subsonic flow and the one of minimization of the input requirements so that only the distribution of speeds V (or equivalently pressures) without further geometric information is sufficient to design the airfoil. The problem of multielement airfoil design and the one of design of airfoils for nonuniform stream conditions should be also studied.

Finally, the successive conformal mapping technique presented here may be an excellent tool for problems where conformal mapping can be used, in particular, in the problem of the generation of structured grids.

Acknowledgment

The author is indebted to J. P. Tamagno and G. A. Raggio for their generous assistance, and to T. Calvi and R. Comes for guidance in the early stages of this work.

References

[1]Lighthill, M. J., "A New Method of Two-Dimensional Aerodynamic Design," British Aeronautical Research Council, R&M 2112, 1945.

[2]Strand, T., "Exact Method of Designing Airfoils with Given Velocity Distributions in Incompressible Flow," *Journal of Aircraft*, Vol. 10, No. 11, 1973, pp. 651–659.

[3]Cohen, M. J., "High-Lift Airfoil Design from the Hodograph," *Journal of Aircraft*, Vol. 21, No. 10, 1984, pp. 760–766.

[4]Volpe, G., "The Inverse Design of Closed Airfoils in Transonic Flow," AIAA Paper 83-504, Jan. 1983.

[5]Liebeck, R. H., and Ormsbee, A. I., "Optimization of Airfoils for Maximum Lift," *Journal of Aircraft*, Vol. 7, No. 5, 1970, pp. 409–415.

[6]Liebeck, R. H., "Subsonic Airfoil Design," *Applied Computational Aerodynamics*, edited by P. A. Henne, Vol. 125, Pt. 3, Progress in Astronautics and Aeronautics, AIAA, Washington, DC and Univ. of Colorado, Boulder, CO, 1990, pp. 133–165, Chap. 5.

[7]Stratford, B. S., "The Prediction of Separation of the Turbulent Boundary Layer," *Journal of Fluid Mechanics*, Vol. 5, Pt. 1, 1959, pp. 1–16.

[8]Limache, A. C., "Diseño de Perfiles Alares de Alta Sustentacion," Trabajo Especial de Licenciatura en Fisica, FaMAF-UNC, March 1992.

[9]Rudin, W., *Real and Complex Analysis*, McGraw–Hill, New York, 1966, pp. 273–275.

[10]Althaus, D., "Profilpolaren für den Modellflug-Windkanalmessunjen an Profilen im kritischen Reynoldszahl-bereich," Neclar-Verlag vs -Villingen, 1980, ISBN 3-7883-0158-9, pp. 80–81.

[11]Anon., "ESDU Transonic Data Memoranda," No. 71020, London, 1971, pp. 11, 12.